RESEARCH ARTICLE
SPACE PHYSICS: SPACE WEATHER

Earth and Planetary Physics
2: 112–119, 2018
doi: 10.26464/epp2018012

A statistical study of the likelihood of a super geomagnetic storm occurring in a mild solar cycle

Bin Zhuang[1*], YuMing Wang[1,2], ChengLong Shen[1,2,3], and Rui Liu[1,3,4]

[1]CAS Key Laboratory of Geospace Environment, Department of Geophysics and Planetary Sciences, University of Science and Technology of China, Hefei 230026, China;

[2]Synergetic Innovation Center of Quantum Information and Quantum Physics, University of Science and Technology of China, Hefei 230026, China;

[3]Mengcheng National Geophysical Observatory, School of Earth and Space Sciences, University of Science and Technology of China, Hefei 230026, China;

[4]Collaborative Innovation Center of Astronautical Science and Technology, Hefei 230026, China

Abstract: The activities of geomagnetic storms are generally controlled by solar activities. The current solar cycle (SC) 24 is found to be mild; compared to SCs 19–23, the storm occurrence and size derived by averaging the occurrence number and D_{st} around the solar maximum are reduced by about 50–82% and 36–61%, respectively. We estimate separately, for SC 19 to 24, the repeat intervals between geomagnetic storms of specific D_{st}, based on fits of power-law and log-normal distributions to the storm data for each SC. Repeat intervals between super geomagnetic storms with $D_{st}\leq$–250 nT are found to be 0.36–2.95 year(s) for SCs 19–23, but about 20 years based on the data for SC 24. We also estimate the repeat intervals between coronal mass ejections (CMEs) of specific speed (V_{CME}) since CMEs are known to be the main drivers of intense storms and the related statistics may provide information about the potential occurrence of super geomagnetic storms from the location of the Sun. Our analysis finds that a CME with $V_{CME}\geq$1860 km/s may occur once per 3 and 5 months in SC 23 and 24, respectively. Based on a V_{CME}-D_{st} relationship, such a fast CME may cause a storm with D_{st}=–250 nT if arriving at the Earth. By comparing the observed geomagnetic storms to storms expected to be caused by CMEs, we derive the probability of CME caused storms, which is dependent on V_{CME}. For a CME faster than 1860 km/s, the probability of a CME caused storm with $D_{st}\leq$–250 nT is about 1/5 for SC 23 or 1/25 for SC 24. All of the above results suggest that the likelihood of the occurrence of super geomagnetic storms is significantly reduced in a mild SC.

Keywords: solar cycle; super geomagnetic storm; repeat interval

Citation: Zhuang, B., Wang, Y. M., Shen, C. L., and Liu, R. (2018). A statistical study of the likelihood of a super geomagnetic storm occurring in a mild solar cycle. *Earth Planet. Phys.*, *2*, 112–119. http://doi.org/10.26464/epp2018012

1. Introduction

Geomagnetic storms, which are disturbances in the magnetic field of the Earth's magnetosphere (e.g., Gonzalez et al., 1994; Tsurutani et al., 1997; Echer et al., 2005), are one category of major space weather events. The size of a geomagnetic storm can be quantified by the corresponding magnetic activity index, e.g., D_{st} index, which is used to distinguish storms of varying severity, such as weak storms with –50 nT<D_{st}<–30 nT, moderate storms with –100 nT<D_{st}<–50 nT, and intense storms with $D_{st}\leq$–100 nT (Gonzalez et al., 1994). Moreover, if a storm is with D_{st}<–250 nT, we call it a super storm, following Astafyeva et al. (2014). Several famous cases have demonstrated that super geomagnetic storms can have significant influence on high-technical systems of modern society, e.g., spacecraft, radio communication, power grid, etc. On 1989 March 14, a geomagnetic storm with $D_{st}\approx$–589 nT (Cliver and Crooker, 1993) struck power systems in Canada and U.S., causing a major power outage for 9 hours in the majority of the Quebec region (Molinski et al., 2000). The "Halloween" event on 2003 October 30 with $D_{st}\approx$–385 nT affected the power system infrastructure, the aviation industry, and satellite communications in Europe and North America (Kappenman, 2005). Tsurutani et al. (2003) reviewed the Carrington event, on 1859 September 1–2, which was the most intense magnetic storm in recorded history with D_{st} estimated to be –1760 nT, and concluded that storms of that extreme strength may occur again. The serious potential hazards of future super storms make it important that the probability of their occurrence be studied (e.g., Borovsky and Denton, 2006; Kataoka and Ngwira, 2016).

Silbergleit (1997) adopted a predictive method of Gumbel's first asymptotic distribution to estimate the repeat interval between storms of specific size, and found that a storm with $D_{st}\leq$–600 nT may occur once per 7 solar cycles (SCs). Tsubouchi and Omura (2007) obtained a repeat interval of about 60 years between storms of $D_{st}\leq$–589 nT by using extreme value theory estimation. Yermolaev et al. (2013) analyzed the standard and integral distribution functions of magnetic storm minimal D_{st} index for the period 1963–2012, and found that the repeat intervals between

Correspondence to: B. Zhuang, zbzb@mail.ustc.edu.cn
Received 04 FEB 2018; Accepted 01 MAR 2018.
Accepted article online 22 MAR 2018.

storms of D_{st}<–500, –1000, and –1500 nT, respectively, are approximately 24, 250 and 1500 years. Love et al. (2015) provided fitting results and corresponding uncertainties for power-law and log-normal distributions of observed storm D_{st} minima for years 1957–2012, and Riley and Love (2017) extended the data analysis to early 2016. However, these studies did not include the storms in SC 24, or included them in combined statistics for SCs 19–24. SC 24 is found to be extremely mild, with storm activities at the lowest level since the 1930s (Gopalswamy, 2012; Richardson, 2013; Gopalswamy et al., 2014). Moreover, SC 25 is predicted to be similar in strength to SC 24 (Cameron et al., 2016; Deminov et al., 2016; Hathaway and Upton, 2016). Accordingly, we study separately the likelihood of occurrence of super geomagnetic storms in a mild SC, and compare results to those observed in previous SCs. In this paper, we will study the repeat intervals between super geomagnetic storms in different SCs. Furthermore, coronal mass ejections (CMEs) are known to be main drivers of intense storms (Gosling et al., 1991; Richardson et al., 2002; Echer et al., 2006; Gonzalez et al., 2007). In order to investigate the likelihood of occurrence of CME caused superstorms we therefore study CME statistics to broaden our view out to the Sun instead of limiting the study to information only at the location of the Earth.

In Section 2, we first compare the occurrence and D_{st} minima of geomagnetic storms in SC 24 with those in SCs 19–23, and then estimate the repeat intervals between storms of specific D_{st}. In Section 3, we study the CMEs in SCs 23 and 24 so as to provide additional information about the occurrence of the potentially CME caused storms. We give the conclusions in Section 4.

2. The Super Geomagnetic Storm Repeat Intervals from Solar Cycle 19 to 24

The World Data Center for Geomagnetism provides geomagnetic storm data online at http://swdcwww.kugi.kyoto-u.ac.jp/index.html. We use the minimal D_{st} index recorded in each day to represent the daily geomagnetic storm size from 1957 January 1 to 2017 December 31. We also download the daily total sunspot number (SSN) record in the same period from the Sunspot Index and Long-term Solar Observations at http://sidc.be/silso/datafiles. First, we show the correlations between the annual count (C_s) and annual D_{st} minima of intense storms with the annually averaged SSN in Figure 1. The correlation coefficients of SSN versus C_s and SSN versus D_{st} are 0.79 and –0.71, respectively. We then display the evolutions of these parameters along SC in Figure 2, in which C_s and D_{st} are found to behave in a similar fashion to SSN. We derive an averaged value of SSN in a SC based on the SSN covering the solar maximum year as well as one year before and after that. However, since there exists a dual-peak storm SC distribution (Gonzalez et al., 1990, 2011; Echer et al., 2011; Le et al., 2013), the averaged C_s and D_{st} in a SC are instead calculated based on some chosen peak values around the solar maximum, shown by the thick blue lines and blue crosses in Figure 2, respectively. These averaged values are listed in Table 1, and used for comparison in

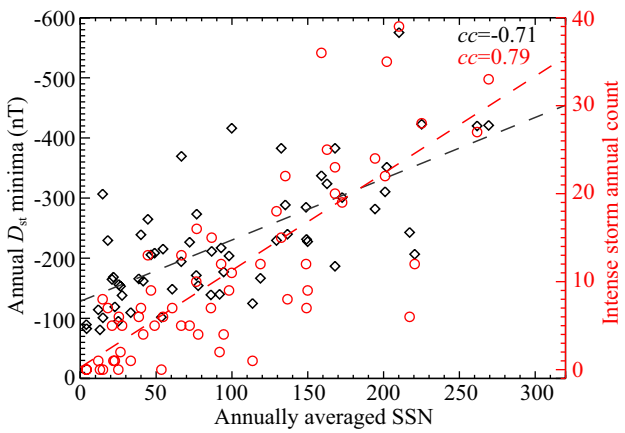

Figure 1. Data points of SSN versus C_s (red circle) and SSN versus D_{st} (black diamond). The dashed lines indicate the linear fits.

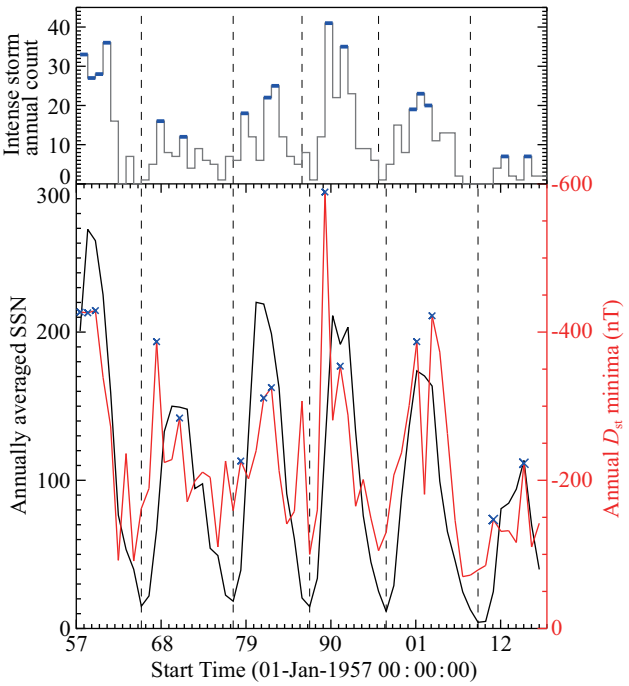

Figure 2. Top: Histogram of the annual count (C_s) of intense geomagnetic storms in SCs 19–24. Bottom: Profile of the annually averaged SSN (black) along with the annual D_{st} minima (red). The period of every SC is indicated by the vertical dashed lines; the blue symbols indicate the chosen C_s and D_{st} peak values.

Table 1. Table of averaged values of the SSN, annual count (C_s) and annual D_{st} minima of intense geomagnetic storms, from SC 19 to SC 24

SC	SSN	C_s	D_{st} (nT)
19	252	31	–427
20	149	14	–335
21	212	22	–287
22	202	38	–471
23	169	21	–404
24	97	7	–185

Note: We average SSN of 1958–1960 in SC 19, 1969–1971 in SC 20, 1980–1982 in SC 21, 1990–1992 in SC 22, 2001–2003 in SC 23, and 2013–2015 in SC 24, respectively.

different SCs by calculating the relative differences between those in SC 24 and those in SC 19 to 23. Overall, comparing SC 24 with SC 19 to 23, there is a decline in SSN of about 35–61%, and C_s and D_{st} are reduced by about 50–82% and 36–61%, respectively.

Figure 3 shows the accumulative histograms of the storm daily D_{st} minima from SC 19 to 24, in which the number of the data points used to construct each bin is the sum of all the data points to the right of itself; the bin size is 10 nT. We then use power-law and log-normal distributions to fit the data points since both distributions can be used to fit storms in terms of frequency versus severity (Love, 2012; Love et al., 2015; Riley and Love, 2017). The equations of the power-law and log-normal distributions are given by equations (1) and (2), respectively, where N is the bin number, and C_1, α, C_2, μ and σ are the fitted parameters:

$$N = C_1|D_{st}|^{-\alpha}, \tag{1}$$

$$N = \frac{C_2}{|D_{st}|}e^{-(\ln|D_{st}|-\mu)^2/2\sigma^2}. \tag{2}$$

We fit the data points for $D_{st}\leq$–50, –100, or –250 nT, and adjust the fitted parameters carefully to make the corresponding reduced chi-square value (χ_ν) close to 1, in which χ_ν is used to test goodness of fit; χ_ν=1 in principle indicates that the estimates best match the observations. The fitted results of the power-law and log-normal distributions are shown by the colored curves in

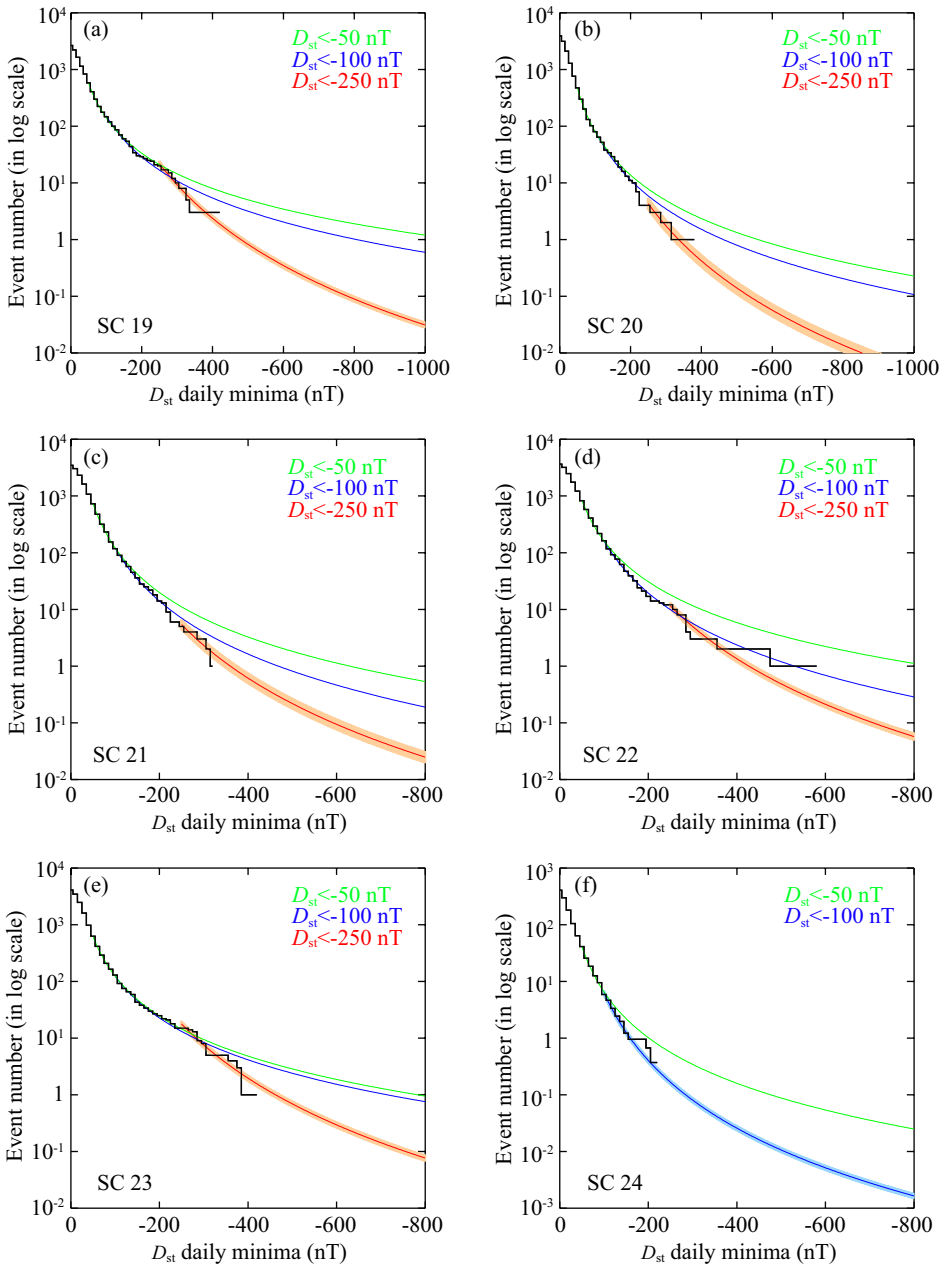

Figure 3. Plot of the accumulative histograms of the storm D_{st} daily minima from SC 19 to 24. The green, blue and red curves indicate the fitted results of the power-law distribution on the data points with $D_{st}\leq$–50, –100 and –250 nT, respectively, while the shadow shows the errors.

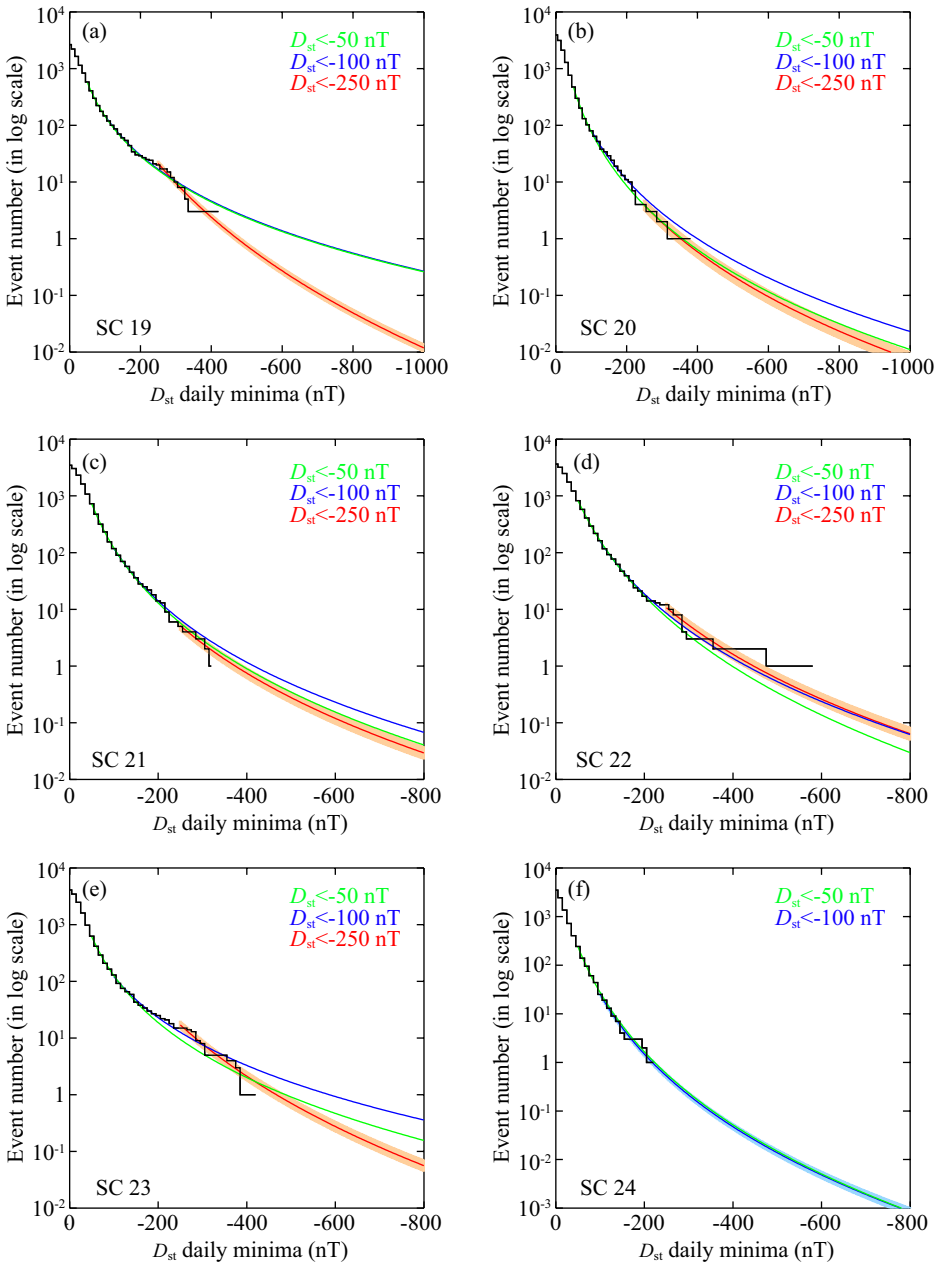

Figure 4. Same as Figure 3 but with the fitted results of the log-normal distribution.

Figure 3 and 4, respectively, and are listed in Table 2. Note that here we can't fit the data points with D_{st}≤–250 nT in SC 24, since the minimum D_{st} in this SC is about –223 nT, which corresponds to the so-called St. Patricks Day event on 2015 March 17 (Kataoka et al., 2015; Wood et al., 2016; Wang et al., 2016). There are several elements to understand in the figures and tables. In Figure 3 of the power-law fit, all the red curves (fitting starting at D_{st}=–250 nT) are beneath the green and blue curves (fitting starting at D_{st}=–50 and –100 nT, respectively), and the blue ones are beneath the green ones. In Figure 4 of the log-normal fit, most of the curves are similar to each other except those in Figure 4a. In Table 2, most of the χ_ν derived by fitting both distributions to the data points with D_{st}≤–250 nT are closest to 1 in SCs 19–23, and χ_ν with D_{st}≤–100 nT is closest to 1 in SC 24. Therefore, to evaluate the data points extended to a smaller D_{st}, we adopt both of the power-law and log-normal distributions to fit the data points, which are started at D_{st}=–250 nT in SC 19 to 23 and at D_{st}=–100 nT in SC 24, respectively. Finally, we can estimate the repeat intervals between storms of D_{st}≤–250, –400 and –600 nT, respectively, where the related interval number at a specific D_{st} is derived by dividing the length of each solar cycle by the corresponding accumulative number of storms in that cycle. The results are listed in Table 3, along with the errors derived by the errors of the fitted data points (shown by the shadow in Figure 3 and 4), which are calculated by the formal 1-sigma errors in each fitted parameter in the solar software (SSW) MPFIT.PRO. From Table 3, we find that storms in SCs 19, 22 and 23 have similar repeat interval numbers, but the numbers in SCs 22 and 23 are slightly larger than those in SC 19. In SCs 20 and 21, with slightly weaker geomagnetic storm activities (see in Table 1 and Figure 2), the estimated storm repeat intervals

Table 2. Table of fitted parameters and their corresponding reduced chi-square values for power-law and log-normal distributions of storms with D_{st}≤–50, –100, and –250 nT, from SC 19 to SC

SC	D_{st}	Power-law		Log-normal	
		Coef (C_1, α)	χ_ν	Coef (C_2, μ, σ)	χ_ν
19	–50	(1.9×10^6, –2.01)	16.11	(14846, 0.32, 1.41)	8.09
	–100	(1.0×10^7, –2.41)	6.35	(10954, 0.57, 1.37)	4.23
	–250	(4.8×10^{12}, –4.73)	1.18	(5062, 2.95, 0.78)	1.14
20	–50	(1.0×10^7, –2.55)	8.19	(11099, 1.16, 1.09)	12.04
	–100	(5.0×10^7, –2.89)	2.56	(5782, 1.36, 1.11)	1.42
	–250	(7.9×10^{11}, –4.70)	1.31	(3154, 1.98, 0.97)	1.02
21	–50	(2.0×10^7, –2.61)	6.34	(12975, 1.14, 1.05)	4.75
	–100	(2.0×10^8, –3.11)	2.73	(25401, 0.80, 1.16)	1.29
	–250	(6.9×10^{11}, –4.03)	1.45	(9920, 1.61, 1.01)	0.66
22	–50	(1.0×10^7, –2.39)	7.72	(3325, 2.45, 0.88)	2.88
	–100	(2.0×10^8, –3.05)	1.66	(6735, 1.86, 1.01)	1.79
	–250	(1.6×10^{12}, –4.65)	1.19	(6934, 2.08, 0.96)	0.60
23	–50	(6.0×10^6, –2.34)	7.26	(14159, 0.86, 1.22)	15.64
	–100	(1.0×10^7, –2.45)	5.39	(8759, 0.70, 1.32)	6.33
	–250	(3.0×10^{12}, –4.68)	1.19	(7041, 2.59, 0.85)	1.11
24	–50	(5.0×10^7, –3.12)	9.45	(3381, 1.93, 0.86)	3.63
	–100	(5.0×10^{10}, –4.63)	1.05	(6163, 1.62, 0.90)	0.43

become approximately ten times those in SCs 19, 22 and 23. Based on data for the mild SC 24, the repeat intervals are much larger than those in the previous SCs, showing that a storm may occur once per 25.3 (19.0), 223 (209) and 1458 (2073) years with D_{st}≤–250, –400 and –600 nT according, respectively, to the power-law (log-normal) distribution fits.

3. The Potential Occurrence of Super Geomagnetic Storms Caused by CMEs

Since CMEs are main drivers of intense geomagnetic storms, the statistics of CMEs can provide additional information about the potential occurrence of super geomagnetic storms from the location of the Sun. The following analysis is based on data from the Large Angle and Spectrometric Coronagraph (LASCO, Brueckner et al., 1995) CME catalog at the Coordinated Data Analysis Workshop Data Center (CDAW, covering data until 2017 April 30; Yashiro et al., 2004; Gopalswamy et al., 2009). As mentioned by Wang and Colaninno (2014), small or faint CMEs could be detected in SC 24 rather than SC 23 because the LASCO image cadence nearly doubled after mid-2010. Therefore, we choose the CDAW/CMEs with speeds higher than 300 km/s and angular widths greater than 30°. Figure 5 shows the accumulative histograms, with bin size set to be 20 km/s, of the considered CMEs as a function of CME speed (V_{CME}) in SCs 23 and 24, and we directly estimate the repeat intervals between CMEs of a specific V_{CME} from the histogram data points. In SC 23, the repeat intervals between CMEs of V_{CME}=1000, 1860 or 2500 km/s are found be 0.3 month, 3 months or 1.3 years, respectively. In SC 24, the corresponding values are 0.7 month, 5 months and 4.7 years.

We will study the likelihood of the occurrence of CME caused storms based on how large the D_{st} would be if a storm was caused by a CME and the probability of a CME arriving at the Earth and causing a storm at that specific D_{st}. Several studies (e.g., Kane, 2005; Yue and Zong, 2011; Gopalswamy et al., 2014) suggested that D_{st} is determined not only by V_{CME} but also by the magnetic fields in the corona and interplanetary space. However, coronagraph observations do not include information about the magnetic fields. Some studies (e.g., Srivastava and Venkatakrishnan, 2002; Gopalswamy et al., 2008; Kilcik et al., 2011) have shown a noteworthy V_{CME}–D_{st} relationship, and thus we use equation (3), which was provided by Gopalswamy et al. (2008), to describe this relationship:

$$D_{st} = -0.1V_{CME} - 64 \ \ (\mathrm{nT}). \tag{3}$$

Equation (3) indicates that a CME with V_{CME}=1860 km/s may cause a geomagnetic storm with D_{st}=–250 nT if arriving at the Earth. We then derive the probability of a CME causing a storm at a specific D_{st} in Figure 6. Figure 6a shows the accumulative histogram (blue) of the expected storms caused by CMEs based on the CME data points in SC 23 as a function of D_{st} which is derived from equation (3), and the accumulative histogram (red) of the observed storms. The blue bin shares the same size as the red one. The ratio of the

Table 3. Estimated repeat intervals (in years) between geomagnetic storms of D_{st}≤–250, –400, and –600 nT

SC	Repeat interval					
	–250 nT		–400 nT		–600 nT	
	PL	LN	PL	LN	PL	LN
19	0.36 (±0.06)	0.37 (±0.04)	3.31 (±0.48)	3.27 (±0.47)	22.8 (±3.4)	29.2 (±4.8)
20	2.68 (±0.78)	2.95 (±0.77)	27.3 (±8.4)	19.6 (±5.9)	204 (±66)	122 (±30)
21	1.82 (±0.46)	1.91 (±0.45)	16.0 (±4.3)	13.1 (±3.5)	106 (±29)	83.3 (±24.3)
22	0.89 (±0.16)	0.96 (±0.23)	7.62 (±1.35)	6.37 (±1.73)	48.8 (±8.9)	39.8 (±9.1)
23	0.66 (±0.09)	0.68 (±0.14)	5.92 (±0.92)	5.48 (±1.26)	39.8 (±6.3)	42.7 (±11.2)
24	25.3 (±3.7)	19.0 (±3.0)	223 (±32)	209 (±35)	1458 (±222)	2073 (±361)

Note: PL and LN indicate the power-law and log-normal distributions, respectively.

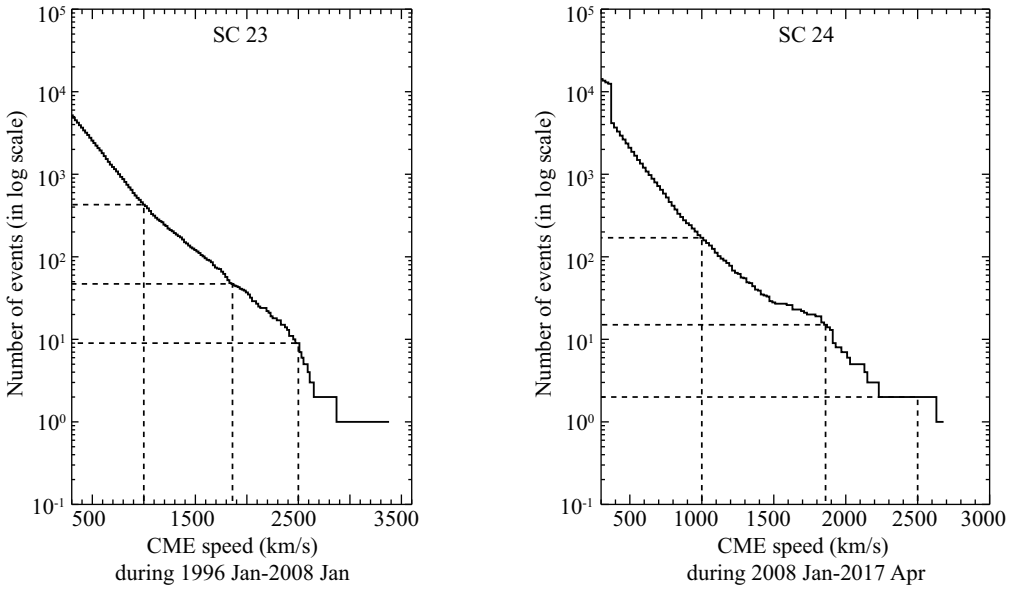

Figure 5. Plot of the accumulative histograms of CMEs as a function of V_{CME} in SC 23 (left) and 24 (right), respectively. The dotted lines indicate that V_{CME}=1000, 1860 and 2500 km/s, and the accumulative numbers at the corresponding speeds.

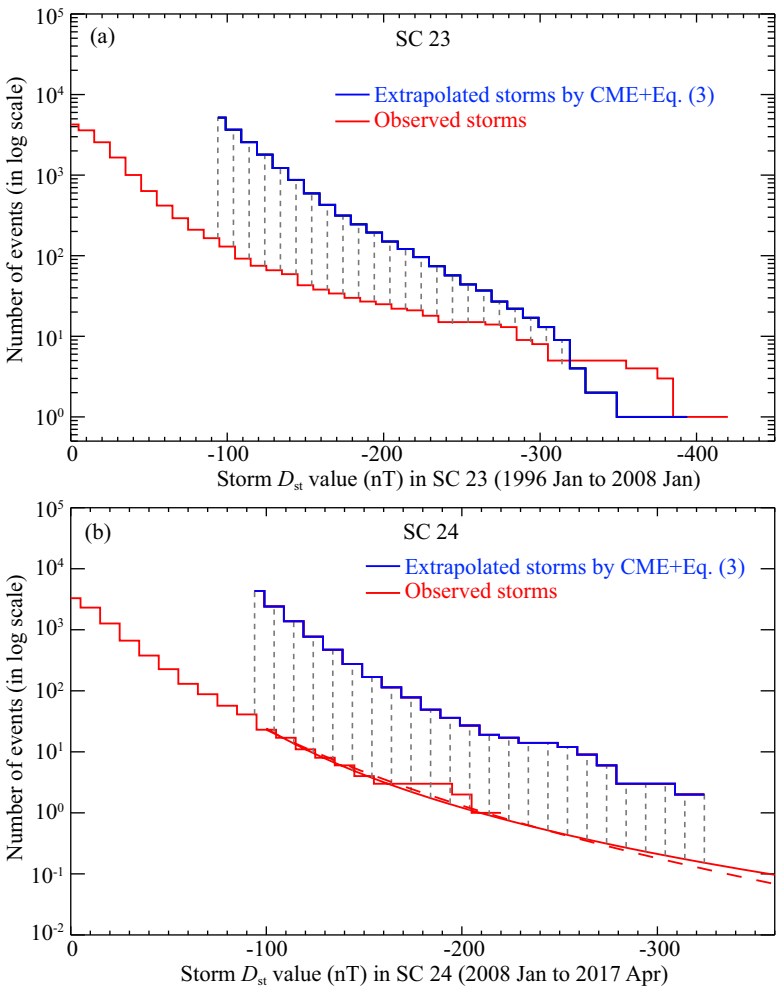

Figure 6. Accumulative histograms of the expected geomagnetic storms caused by CMEs (blue), as a function of D_{st} and the observed geomagnetic storms (red) in SC 23 (a) and SC 24 (b), respectively. The vertical dotted lines indicate the values of 1/*P*. In panel (b), the red solid (dashed) curve indicates the fitted data points by the power-law (log-normal) distribution.

red data points to the blue data points, P, gives the probability of a CME causing a storm. Note that here the location of the blue bin may not match perfectly with that of the red bin, so P is calculated by dividing the red bin number by the number of the blue data point that is closest to the red one. P is found to be about 1/35 at V_{CME}=300 km/s, but as high as 1/5 or 1/2 at V_{CME}=1860 or 2500 km/s, respectively. In Figure 6a, the blue line crosses the red line at D_{st}≈–320 nT. It may be that equation (3) underestimates the D_{st} of severe storms (refer to Figure 5a in Gopalswamy et al. (2008)), but it still makes sense to use equation (3) to compare relatively the likelihoods of occurrence of CME caused storms in different SCs. Similarly, we estimate P in SC 24 in Figure 6b according to the corresponding CME data points and equation (3). Here we use the fitted data points of the power-law and log-normal distributions to represent the observed storms whose D_{st} are smaller than –223 nT. P is found to be about 1/110 at V_{CME}=300 km/s, and the power-law distribution fit gives P≈1/25 at V_{CME}=1860 km/s and P≈1/12 at V_{CME}=2500 km/s, respectively, while the other fit gives the related P to be between 1/26 and 1/15. Overall, P is found to be dependent on V_{CME}, and larger in SC 23 than in SC 24, which may indicate that the magnetic field strength determining the storm D_{st} is a function of P.

4. Conclusions and Discussions

In this paper, we study the likelihood of the occurrence of super geomagnetic storms in a mild SC. First, we find that the storm occurrence and size, which are derived by averaging the annual occurrence number and annual D_{st} minima of intense storms around the solar maximum, are reduced by about 50–82% and 36–61% in SC 24 compared to those in SCs 19 to 23, respectively. We then evaluate the repeat interval between super storms of specific D_{st} by fits of power-law and log-normal distributions. We apply both fits to the storm data points with D_{st}≤–50, –100 or –250 nT in SC 19 to 23, and find that the fits starting at D_{st}=–250 nT give the most reliable results, as confirmed by minimum chi-square values. In SC 24, the results are based on the storm data points with D_{st}≤ –100 nT. This analysis finds that estimated repeat intervals of super geomagnetic storms in SC 24 are much larger than those in SCs 19–23, e.g., the fits of the power-law and log-normal distributions give the repeat interval between storms of D_{st}≤–250 nT close to 20 years for SC 24 compared to less than 3 years for the previous 5 SCs. We also study the statistics of the CME occurrences in SCs 23 and 24. We find that a CME with V_{CME}=1860 km/s may occur once per 3 or 5 months in SC 23 and 24, respectively. According to a V_{CME}–D_{st} relationship, such a fast CME may cause a storm with D_{st}=–250 nT if arriving at the Earth. By comparing the observed geomagnetic storms with the expected storms caused by CMEs, we derive the probability of a CME causing a storm, which is dependent on V_{CME}. For a CME faster than 1860 km/s, the probability of the CME causing a storm with D_{st} less than –250 nT is 1/5 for SC 23 or around 1/25 for milder SC 24. All of the above results suggest that the likelihood of a super geomagnetic storm is significantly reduced in a mild SC. The upcoming SC 25, which is predicted to be as mild as SC 24, can be used to test these results.

Acknowledgments

We acknowledge and thank the World Data Center for Geomagnetism (Kyoto) for use of the geomagnetic storm D_{st} database, and the Royal Observatory of Belgium (ROB) for use of sunspot number data. The CME catalog is generated and maintained at the CDAW Data Center by NASA and the Catholic University of America in cooperation with the Naval Research Laboratory. This work is supported by grants from NSFC (41774178, 41574165, 41421063, and 41274173), and the fundamental research funds for the central universities.

References

Astafyeva, E., Yasyukevich, Y., Maksikov, A., and Zhivetiev, I. (2014). Geomagnetic storms, super-storms, and their impacts on GPS-based navigation systems. *Space Wea.*, *12*(7), 508–525. https://doi.org/10.1002/2014SW001072

Borovsky, J. E., and Denton, M. H. (2006). Differences between CME-driven storms and CIR-driven storms. *J. Geophys. Res. Space Phys.*, *111*(A7), A07S08. https://doi.org/10.1029/2005JA011447

Brueckner, G. E., Howard, R. A., Koomen, M. J., Korendyke, C. M., Michels, D. J., Moses, J. D., Socker, D. G., Dere, K. P., Lamy, P. L., … Eyles, C. J. (1995). The large angle spectroscopic coronagraph (LASCO). *Solar Phys.*, *162*(1-2), 357–402. https://doi.org/10.1007/BF00733434

Cameron, R. H., Jiang, J., and Schüssler, M. (2016). Solar cycle 25: another moderate cycle?. *Astrophys. J.*, *823*(2), L22. https://doi.org/10.3847/2041–8205/823/2/L22

Cliver, E. W., and Crooker, N. U. (1993). A seasonal dependence for the geoeffectiveness of eruptive solar events. *Solar Phys.*, *145*(2), 347–357. https://doi.org/10.1007/BF00690661

Deminov, M. G., Nepomnyashchaya, E. V., and Obridko, V. N. (2016). Properties of solar activity and ionosphere for solar cycle 25. *Geomagn. Aeronomy*, *56*(6), 742–749. https://doi.org/10.1134/S0016793216060086

Echer, E., Gonzalez, W. D., Guarnieri, F. L., Lago, A. D., and Vieira, L. E. A. (2005). Introduction to space weather. *Adv. Space Res.*, *35*(5), 855–865. https://doi.org/10.1016/j.asr.2005.02.098

Echer, E., Gonzalez, W. D., and Alves, M. V. (2006). On the geomagnetic effects of solar wind interplanetary magnetic structures. *Space Wea.*, *4*(6), 1–11. https://doi.org/10.1029/2005SW000200

Echer, E., Gonzalez, W. D., and Tsurutani, B. T. (2011). Statistical studies of geomagnetic storms with peak D_{st} ≤ –50 nT from 1957 to 2008. *J. Atmos. Solar Terr. Phys.*, *73*(11-12), 1454–1459. https://doi.org/10.1016/j.jastp.2011.04.021

Gonzalez, W. D., Gonzalez, A. L. C., and Tsurutani, B. T. (1990). Dual-peak solar cycle distribution of intense geomagnetic storms. *Planet. Space Sci.*, *38*(2), 181–187. https://doi.org/10.1016/0032-0633(90)90082-2

Gonzalez, W. D., Joselyn, J. A., Kamide, Y., Kroehl, H. W., Rostoker, G., Tsurutani, B. T., Vasyliunas, V. M. (1994). What is a geomagnetic storm?. *J. Geophys. Res.*, *99*(A4), 5771–5792. https://doi.org/10.1029/93JA02867

Gonzalez, W. D., Echer, E., Clua-Gonzalez, A. L., and Tsurutani, B. T. (2007). Interplanetary origin of intense geomagnetic storms (D_{st} < –100 nT) during solar cycle 23. *Geophys. Res. Lett.*, *34*(6), L06101. https://doi.org/10.1029/2006GL028879

Gonzalez, W. D., Echer, E., de Gonzalez, A. L. C., Tsurutani, B. T., and Lakhina, G. S. (2011). Extreme geomagnetic storms, recent Gleissberg cycles and space era-superintense storms. *J. Atmos. Solar Terr. Phys.*, *73*(11-12), 1447–1453. https://doi.org/10.1016/j.jastp.2010.07.023

Gopalswamy, N., Akiyama, S., Yashiro, S., Michalek, G., and Lepping, R. P. (2008). Solar sources and geospace consequences of interplanetary magnetic clouds observed during solar cycle 23. *J. Atmos. Solar Terr. Phys.*, *70*(3-4), 245–253. https://doi.org/10.1016/j.jastp.2007.08.070

Gopalswamy, N., Yashiro, S., Michalek, G., Stenborg, G., Vourlidas, A., Freeland, S., Howard, R. (2009). The SOHO/LASCO CME catalog. *Earth Moon Planets*, *104*(1-4), 295–313. https://doi.org/10.1007/s11038-008-9282-7

Gopalswamy, N. (2012). Energetic particle and other space weather events of solar cycle 24. In Proceedings of the 11th Annual Astrophysical Conference (Vol. 1500, pp. 14–19). Palm Springs, CA: American Institute of Physics. https://doi.org/10.1063/1.4768738

Gopalswamy, N., Akiyama, S., Yashiro, S., Xie, H., Mäkelä, P., Michalek, G. (2014). Anomalous expansion of coronal mass ejections during solar cycle 24 and its space weather implications. *Geophys. Res. Lett.*, *41*(8), 2673–2680. https://doi.org/10.1002/2014GL059858

Gosling, J. T., McComas, D. J., Phillips, J. L., and Bame, S. J. (1991). Geomagnetic activity associated with earth passage of interplanetary shock disturbances and coronal mass ejections. *J. Geophys. Res. Space Phys.*, *96*(A5), 7831–7839. https://doi.org/10.1029/91JA00316

Hathaway, D. H., and Upton, L. A. (2016). Predicting the amplitude and hemispheric asymmetry of solar cycle 25 with surface flux transport. *J. Geophys. Res. Space Phys.*, *121*(11), 10744–10753. https://doi.org/10.1002/2016JA023190

Kane, R. P. (2005). How good is the relationship of solar and interplanetary plasma parameters with geomagnetic storms?. *J. Geophys. Res. Space Phys.*, *110*(A2), A02213. https://doi.org/10.1029/2004JA010799

Kappenman, J. G. (2005). An overview of the impulsive geomagnetic field disturbances and power grid impacts associated with the violent Sun-Earth connection events of 29–31 October 2003 and a comparative evaluation with other contemporary storms. *Space Wea.*, *3*(8), s08C01. https://doi.org/10.1029/2004SW000128

Kataoka, R., Shiota, D., Kilpua, E., and Keika, K. (2015). Pileup accident hypothesis of magnetic storm on 17 March 2015. *Geophys. Res. Lett.*, *42*(13), 5155–5161. https://doi.org/10.1002/2015GL064816

Kataoka, R., and Ngwira, C. (2016). Extreme geomagnetically induced currents. *Progr. Earth Planet. Sci.*, *3*(1), 23. https://doi.org/10.1186/s40645-016-0101-x

Kilcik, A., Yurchyshyn, V. B., Abramenko, V., Goode, P. R., Gopalswamy, N., Ozguc, A., Rozelot, J. P. (2011). Maximum coronal mass ejection speed as an indicator of solar and geomagnetic activities. *Astrophys. J.*, *727*(1), 44. https://doi.org/10.1088/0004-637X/727/1/44

Le, G. M., Cai, Z. Y., Wang, H. N., Yin, Z. Q., and Li, P. (2013). Solar cycle distribution of major geomagnetic storms. *Res. Astron. Astrophys.*, *13*(6), 739–748. https://doi.org/10.1088/1674-4527/13/6/013

Love, J. J. (2012). Credible occurrence probabilities for extreme geophysical events: Earthquakes, volcanic eruptions, magnetic storms. *Geophys. Res. Lett.*, *39*(10), L10301. https://doi.org/10.1029/2012GL051431

Love, J. J., Rigler, E. J., Pulkkinen, A., and Riley, P. (2015). On the lognormality of historical magnetic storm intensity statistics: Implications for extreme-event probabilities. *Geophys. Res. Lett.*, *42*(16), 6544–6553. https://doi.org/10.1002/2015GL064842

Molinski, T. S., Feero, W. E., and Damsky, B. L. (2000). Shielding grids from solar storms [power system protection]. *IEEE Spectr.*, *37*(11), 55–60. https://doi.org/10.1109/6.880955

Richardson, I. G., Cane, H. V., and Cliver, E. W. (2002). Sources of geomagnetic activity during nearly three solar cycles (1972-2000). *J. Geophys. Res. Space Phys.*, *107*(A8), 1187. https://doi.org/10.1029/2001JA000504

Richardson, I. G. (2013). Geomagnetic activity during the rising phase of solar cycle 24. *J. Space Wea. Space Climate*, *3*(11), A08. https://doi.org/10.1051/swsc/2013031

Riley, P., and Love, J. J. (2017). Extreme geomagnetic storms: Probabilistic forecasts and their uncertainties. *Space Wea.*, *15*(1), 53–64. https://doi.org/10.1002/2016SW001470

Silbergleit, V. M. (1997). On the occurrence of the largest geomagnetic storms per solar cycle. *J. Atmos. Solar Terr. Phys.*, *59*(2), 259–262. https://doi.org/10.1016/S1364-6826(96)00002-8

Srivastava, N., and Venkatakrishnan, P. (2002). Relationship between CME speed and geomagnetic storm intensity. *Geophys. Res. Lett.*, *29*(9), 1-1–1-4. https://doi.org/10.1029/2001GL013597

Tsubouchi, K., and Omura, Y. (2007). Long-term occurrence probabilities of intense geomagnetic storm events. *Space Wea.*, *5*(12), 1–12. https://doi.org/10.1029/2007SW000329

Tsurutani, B. T., Gonzalez, W. D., Kamide, Y., and Arballo, J. K. (1997). Magnetic Storms. Washington DC: American Geophysical Union. https://doi.org/10.1029/GM098p00ix

Tsurutani, B. T., Gonzalez, W. D., Lakhina, G. S., and Alex, S. (2003). The extreme magnetic storm of 1-2 September 1859. *J. Geophys. Res. Space Phys.*, *108*(A7), 1268. https://doi.org/10.1029/2002JA009504

Wang, Y. M., and Colaninno, R. (2014). Is solar cycle 24 producing more coronal mass ejections than cycle 23?. *Astrophys. J. Lett.*, *784*(2), L27. https://doi.org/10.1088/2041-8205/784/2/L27

Wang, Y. M., Zhang, Q. H., Liu, J. J., Shen, C. L., Shen, F., Yang, Z. C., Zic, T., Vrsnak, B., Webb, D. F., … Bin, Z. (2016). On the propagation of a geoeffective coronal mass ejection during 15–17 March 2015. *J. Geophys. Res. Space Phys.*, *121*(8), 7423–7434. https://doi.org/10.1002/2016JA022924

Wood, B. E., Lean, J. L., McDonald, S. E., and Wang, Y. M. (2016). Comparative ionospheric impacts and solar origins of nine strong geomagnetic storms in 2010–2015. *J. Geophys. Res. Space Phys.*, *121*(6), 4938–4965. https://doi.org/10.1002/2015JA021953

Yashiro, S., Gopalswamy, N., Michalek, G., Cyr, O. C. S., Plunkett, S. P., Rich, N. B., Howard, R. A. (2004). A catalog of white light coronal mass ejections observed by the SOHO spacecraft. *J. Geophys. Res. Space Phys.*, *109*(7), A07105. https://doi.org/10.1029/2003JA010282

Yermolaev, Y. I., Lodkina, I. G., Nikolaeva, N. S., and Yermolaev, M. Y. (2013). Occurrence rate of extreme magnetic storms. *J. Geophys. Res. Space Phys.*, *118*(8), 4760–4765. https://doi.org/10.1002/jgra.50467

Yue, C., and Zong, Q. G. (2011). Solar wind parameters and geomagnetic indices for four different interplanetary shock/ICME structures. *J. Geophys. Res. Space Phys.*, *116*(A12), A12201. https://doi.org/10.1029/2011JA017013